Investigation of third body role in dry contacts: Experimental procedure to dissociate the effects of substrate and interface layer on the contact pair frictional response

Simone Ciprari, Valentin Ripard, Aurélien Saulot, Francesco Massi

Tribology International 190 (2023) 109047

Contents lists available at ScienceDirect

Tribology International

journal homepage: www.elsevier.com/locate/triboint

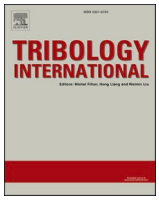

Investigation of third body role in dry contacts: Experimental procedure to dissociate the effects of substrate and interface layer on the contact pair frictional response

Simone Ciprari [a,b,c,*], Valentin Ripard [c], Aurélien Saulot [b], Francesco Massi [a]

[a] Department of Mechanical and Aerospace Engineering, Sapienza University of Rome, Rome, Italy
[b] Univ. Lyon, INSA Lyon, CNRS, LAMCOS, UMR5259, 69621 Villeurbanne, France
[c] Safran Landing Systems, 69100 Villeurbanne, France

ARTICLE INFO

Keywords:
Friction
Third body
Rheology
Dry contact

ABSTRACT

This paper presents an experimental approach for the evaluation of the third body role in dry contacts. The ultrasonic cleaning is applied to remove the third body layer from a contact sample pair, allowing to perform frictional tests with and without the interface layer. The comparison between the observed behaviors evidences a strong influence of the third body on the overall frictional response. The cleaned samples have been used as the substrate to introduce an external third body. The frictional tests pointed out the predominant role of the interface layer, rather than the substrate, on the frictional performances. This procedure allows to test external (eventually artificial) third bodies, investigating the role of different features (morphology, composition) on the frictional response.

1. Introduction

The study of the third body layer in terms of its effect on the frictional performances is one of the main topics of interest in tribology. The concept of third body has been firstly introduced by Godet in the 1970s [1], as a contact entity that provides the separation of the first bodies in contact, with the aim to clarify the load transmission and the velocity accommodation. The concept has been extended by Berthier, that proposed the third body as one of five possible sites in which relative velocity can be accommodated in a mechanical system [2]. Berthier also evidenced the importance of third body rheology inside the contact interface, introducing the concepts of tribological circuit and tribological flows, redefining the wear as the flow of matter that permanently leaves the contact interface [2].

In dry contacts, the rheology of the third body results to be extremely complex, due to the discontinuity and evolutive characters of such a complex media, which is subjected to high local stress and strain rates. The question of establishing a parallelism between a solid third body and a fluid one (lubricant) has been afforded since the 1980s [3], but the problem has still no solution. In fact, differently from a fluid lubricant, the rheology of a solid third body is not directly describable by a constitutive law and the material cannot be described by an exhaustive parameter, as the viscosity does for a lubricant [4–6]. Moreover, in presence of a solid third body, the boundary conditions strongly depend on the first bodies surface chemistry and topography [7]. The evolutive and discontinue chemical and morphological characteristics of the third body at the interface increase the complexity in understanding and predicting. Nevertheless, numerical and analytical simulations have been attempted to simulate the role of third body features in simple normal contacts [8], or even for tangentially loaded contacts, as for instance in [5,9]. By an experimental point of view, because of the discontinuity and non-homogeneous character of this layer, largely affected by several mechanical and physio-chemical phenomena, there are not well-established experimental procedures to directly evaluate its rheology and effects on a dry contact. One of the main issues, is to separate the contribution of the third body from the ones coming from the bodies in contact and their surfaces.

The understanding of the third body rheology and its role at the very local scale is strongly linked with the global frictional response at the macro scale and, therefore, with the system aptitude to incurs in self-excited friction-induced vibrations [10–13]. Different unstable mechanism, related to different frictional behavior of the contact pair, can lead to the occurrence of such unstable oscillations in braking systems, as mode coupling [14,15], negative friction-velocity slope [16,17] or

* Corresponding author at: Department of Mechanical and Aerospace Engineering, Sapienza University of Rome, Rome, Italy.
E-mail address: simone.ciprari@uniroma1.it (S. Ciprari).

https://doi.org/10.1016/j.triboint.2023.109047
Received 15 September 2023; Received in revised form 16 October 2023; Accepted 24 October 2023
Available online 27 October 2023

stick-slip [18,19]. Being such instabilities originated at the frictional interface, the role of the third body layer on the local and macroscopic frictional response of contact systems is directly related to the occurrence of either stable or unstable friction-induced vibrations [12,18].

Carbon/Carbon (C/C) composites materials are considered to be one of the most suitable in high performance frictional applications, because of low density, high mechanical strength and thermal stability [20–23]. For this reason, C/C materials have been here chosen to develop a new approach for investigating the specific role of the third body layer in the overall frictional and vibration response of a contact system. Because of their industrial interest, C/C have been the object of several experimental works, that characterized their tribological performance in function of different operating parameters (sliding velocity, normal load, temperature) and environmental conditions [24–28], as well as their aptitude to induce dynamic contact instabilities [29,30]. Many studies focused also on the characterization of wear debris [31–33] generated during the sliding contact, mainly with the aim of understanding the wear mechanism affecting the C/C materials [34].

In this context, this work aims to propose an experimental approach to evaluate, indirectly, the role of the third body in the overall frictional response of a dry contact. The procedure has been here applied to the contact between Carbon/Carbon (C/C) composites materials.

2. Materials and method

The proposed approach has been developed to investigate the role of the third body layer in the frictional response of material pairs, on a dedicated tribometer. The main steps of this approach consist in:

1. Testing friction pairs coming from a specific application, with a third body layer well established, directly in-situ, during the frictional contact in real operative conditions; this first step allow for obtaining a reference frictional response of the material pair.
2. Cleaning the contact samples by ultrasonic cleaning, allowing for removing, collecting and analyzing the third body removed from the interface.
3. Testing the contact pairs without third body, previously removed, to investigate their frictional response.
4. Re-introducing the third body on the contact pair surfaces. The third body could be either the one previously collected, or artificial third body created or recovered from other contact pairs.
5. Testing the samples with the reintroduced-third body layer and comparing their frictional response with the one of the cleaned samples and the original ones.

In this section, firstly, the test bench and the material samples are presented. Then, cleaning and re-introduction procedures of the third body layer are presented.

2.1. Experimental set-up

The experimental campaign has been performed on a specific test bench, named TriboAir (Fig. 1), used to study the frictional response of the analyzed material samples and the associated vibrational response. This tribometer has been designed to have a simple dynamics, allowing to investigate the dynamic excitation generated at the interface [35,36] and the overall frictional and vibrational response, in well controlled boundary conditions and reduced external parasitic perturbations.

The TriboAir test bench is a linear tribometer, therefore, a reciprocating relative motion is imposed between the samples by a linear voice coil motor ((8), BEI KIMCO LA30–75–001A), coupled with an optical encoder (MicroE OPS-200–1–1) and a controller (Elmo G-DCWHI10/100EE). The use of this kind of motor, in combination with the use of air bearings (1), allows to have the moving part completely suspended in air, resulting in the reduction of external parasitic noise that could affect the measurement, as well as in a better control of the boundary conditions. The load as well is imposed by dead weights driven by air bearings. The only contact interface in relative motion, therefore, is the one between the samples (3), that is the only source of friction-induced vibrations.

This test bench allows the imposition of different motion and temperature laws, this latter ensured using InfraRed (IR) lamps (2) driven by a PID controller (GEFRAN F650). The measurement of the temperature,

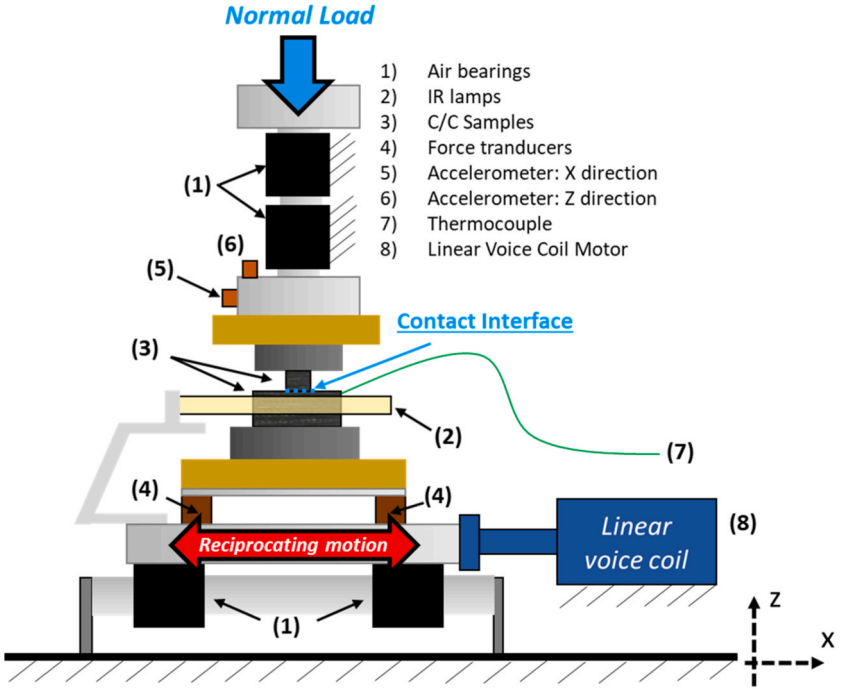

Fig. 1. TriboAir test bench functional scheme. The main components of the Test bench have been evidenced: 1) Air Bearings, 2) IR Lamps, 3) C/C Samples, 4) Force Transducers, 5) Accelerometer X Direction, 6) Accelerometer Z Direction, 7) Thermocouple, 8) Linear Voice Coil Motor.

necessary also to feedback the controller, is performed by a thermocouple (7) placed in a hole drilled 3 millimeters below the contact interface. For the present work a contact pressure representative of the contact conditions encountered in the real application is imposed by dead weights.

The dynamic response (friction-induced vibrations) of the system to the dynamic excitation generated at the contact interface is registered by two accelerometers along the tangential (5) and normal (6) directions to the contact. The contact forces are registered by two tri-axials piezoelectric force transducers (Kistler 9017C).

All data are recorded by an acquisition system SIRIUSi - DEWESOFT, based on DualCoreADC® technology with dual 24-bit delta-sigma analog to digital converter (ADC), with a sampling frequency equal to 40 kHz, and then post-processed by MATLAB ©.

2.2. Contact material samples

The C/C specimens, used in the present investigation, have been directly machined from brake discs, demounted after service life on a real braking apparatus, therefore, with a natural and well established third body layer. Fig. 2 provides an example of the machined samples used in the experimental campaign. Upper views of the frictional surfaces are also shown.

As shown in Fig. 2, a simple geometry has been adopted for the used specimens, with the aim of simplify their own dynamics, while controlling the contact parameters.

2.3. Ultrasonic cleaning procedure

The Ultrasonic (US) Cleaning is a widely used technique in many research and industrial applications [37]. So far, in the field of tribology, it has been used in various applications, for instance to prepare samples surfaces [38–40], to study the effect of transfer layer on wear rate [41], to disperse additives inside lubricants [42], etc. In this work, this technique is directly used to remove a solid third body from the contact surface and superficial open porosities, that could act as a reservoir for the third body recirculating in the contact.

A synthetic scheme of the adopted setup is shown in Fig. 3.

As shown in Fig. 3, only the frictional surface of the sample is submerged into the solvent, to minimize the portion of the sample in contact with the liquid and avoiding contaminations form the sides of the sample. In this way, only the frictional surface is cleaned, allowing to minimize the impact on first body. The use of the term “solvent” is

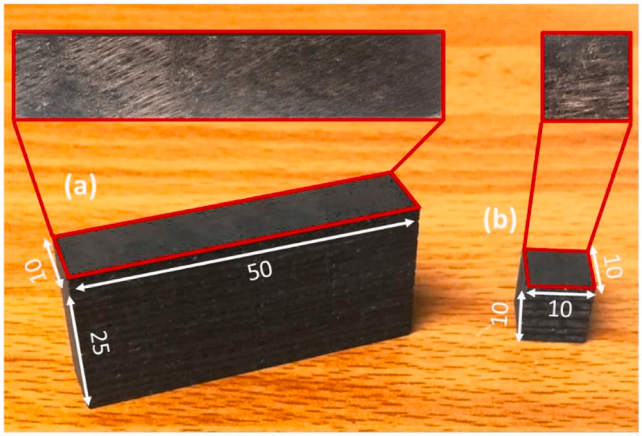

Fig. 2. Example of specimens used in the experimental campaign. The lower specimen (a) is a 50×10×25 mm prism, the upper specimen (b) is a cube with 10 mm edge. A detail of frictional surfaces is also provided. The adjectives “lower” and “upper” are referred to their position in the set-up configuration shown in Fig. 1.

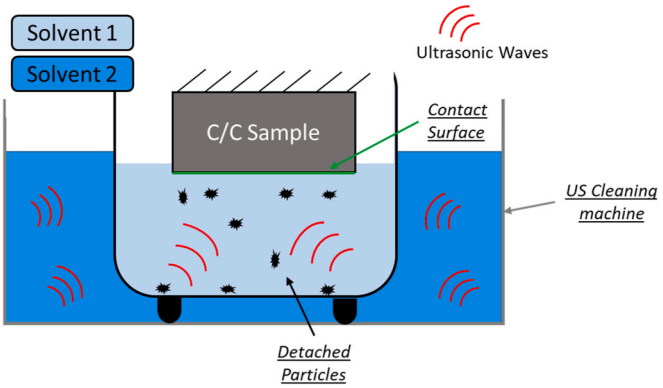

Fig. 3. Ultrasonic Cleaning set-up.

knowingly improper in this application, because no chemical solutions are involved. This nomenclature has been adopted to refers to the dispersion of detached third body particles inside the “solvent 1″, observed after the cleaning procedure. The ultrasonic cleaning, lasting 15 min with a sinusoidal wave profile at 40 kHz, is followed by a phase of sample drying, performed under vacuum (≈ 5 Pa) for at least 48 h, to degage from the surfaces the used solvent, minimizing its effect on the successive frictional tests. The samples are restored for two hours in ambient air before the successive frictional tests.

In this work, distilled water has been used as the “Solvent 1″, because of the presence of water in the material operating environment, avoiding in this way to introduce a further fluid that would have led to unrealistic physiochemical reactions. Common water was used as “Solvent 2″, having the only function of acting as the media by which ultrasonic waves are transmitted from the machine towards the sample. The choice of using two different and separated solvents has been adopted to facilitate the collection of detached third body, used for observations and tests after the evaporation of the solvent.

The effectiveness of the experimental procedure has been verified by scanning electron microscope (SEM), observing the same zones of the sample frictional surface before and after the process of ultrasonic cleaning. An example of the acquired images is reported in Fig. 4. As can be observed, the ultrasonic cleaning process removed most of the third body that was on the frictional surface and inside the porosities, without causing damage to the first body. Consequently, two main conditions can be achieved by the ultrasonic cleaning. Firstly, the same sample pair can be tested with and without the presence of the interface layer, allowing for a direct comparison. Secondly, a substrate representative of the used material, cleaned from its original third body, is available to introduce an external / artificial third body.

The ultrasonic cleaning set-up allows for a simple collection of the third body detached from surface and porosities, that is directly available to be observed, as shown in Fig. 5, that present an example of SEM observation performed on the recovered third body.

2.4. Third body reintroduction

The third body reintroduction procedure has been set in place with the objective of being able to test an external / artificial third body, distinguishing between its role and the one of the original substrate (first body). The reintroduced third body could be either retrieved from a used disc, and so representative of the material state during the real application, or artificially constituted to investigate the role of specific constituents.

A scheme of the procedure is reported in Fig. 6. It is composed by the following three main steps, which can be repeated if retained necessary:

i. Firstly, the external third body, object of the test, is deposed on the frictional surface of the sample, that has been previously

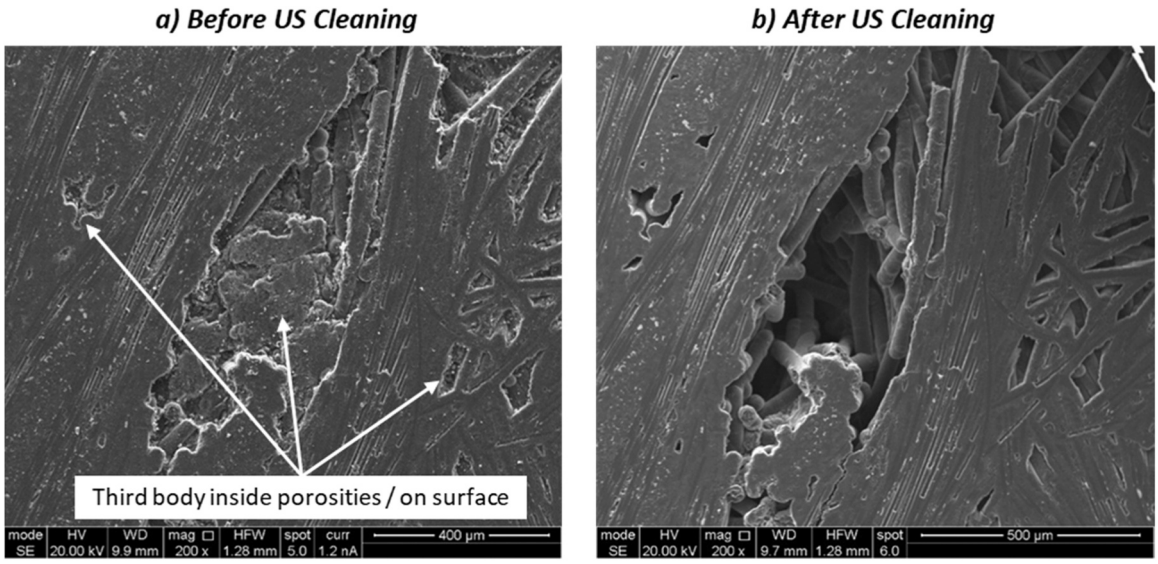

Fig. 4. SEM Images acquired on the same zone of sample frictional surface: Before (a) and After (b) ultrasonic cleaning process.

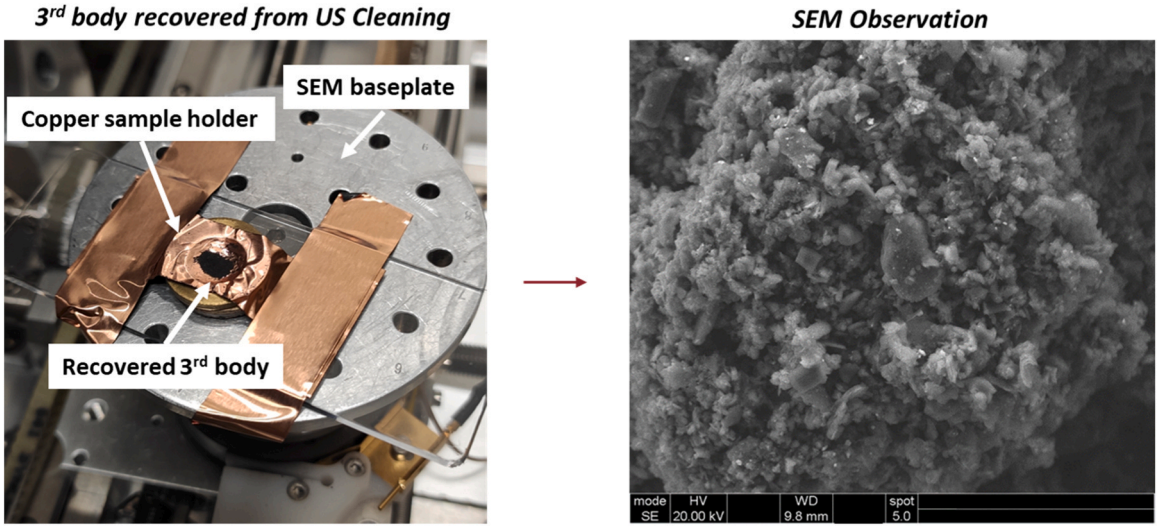

Fig. 5. Example of SEM observation on third body recovered from ultrasonic cleaning. In the left image recovered third body is recognizable as a black pile on the copper support.

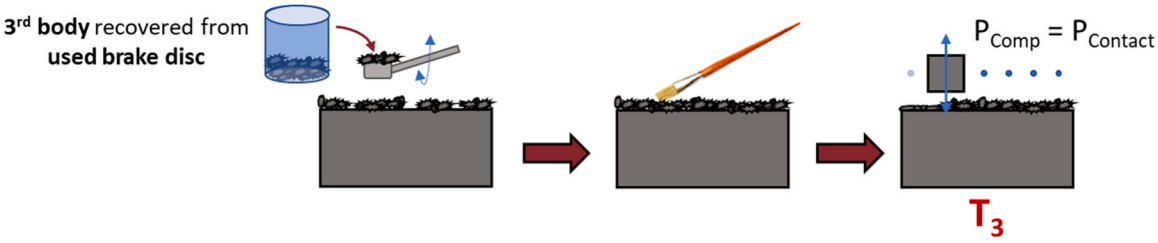

Fig. 6. Scheme of the third body reintroduction procedure. Three different steps have been applied. 1) Deposition of the external / artificial third body on the sample surface 2) Distribution of the third body by the use of a brush 3) Third body compaction at high temperature, applying the same pressure of the one used during braking.

cleaned with the described ultrasonic procedure. The amount of third body deposed on the surface has been measured to be around 3 milligrams.

ii. The deposed third body is far from being uniformly distributed on the entire surface. To approach a uniform distribution, a brush is used to distribute the deposed powder on the surface.

iii. As a last step, as described in Fig. 6, the system is heated up to the service life working temperature (referred as T_3 in the following), while a normal load, calculated to have the same contact pressure used in operative conditions, is applied statically to compact the third body on the surfaces, without the application of any relative motion between the two samples in contact. The contact pressure is applied along all the surface by unloading, moving and

reloading the samples. The temperature has been set to be representative of real temperature ranges in the real application.

After cooling down to room temperature, a running-in phase is performed, imposing a sliding motion between the samples for 30 min. This last step allowed to expel the excess of reintroduced third body, approaching a surface and porosity redistribution of the third body closer to the one originated by the operative sliding conditions. The samples are then ready to be tested on the tribometer.

3. Experimental tests

To evaluate the role of the third body on the frictional response of the investigated C/C contact pair, the same samples have been tested in different states. The reference test has been conducted on the samples in the original state, directly machined from a brake disc demounted after service life. This state will be referred in the following as "Before US" and represent the reference state of the contact pair. The samples, then, have been cleaned by ultrasonic cleaning, as described in 2.3, to remove the third body layer, this state is indicated as "After US". In a successive step, third body recovered from a different brake disc, made of the same material, has been reintroduced on the cleaned sample (state referred as "After Reintroduction"). This sequence allows for a direct comparison between successive tests, always performed with the same first bodies, permitting to evaluate the effect of the third body layer on the frictional response, with respect to cleaned C/C samples, or the effect on the same ones of an external reintroduced third body.

3.1. Test protocol

Reciprocating sliding is provided by the TriboAir tribometer, under a contact pressure representative of the real application. The tribological and dynamic response of a C/C contact pair has been proved to be strongly dependent on the imposed conditions [24,26,29]. Therefore, it is necessary to define and apply a well-defined test protocol, in terms of sliding velocity and temperature conditions.

As concerns the sliding velocity, a variable velocity motion law is imposed, as described in Fig. 7. This motion law has been chosen to maximize the decreasing velocity part of each stroke, simulating a braking event. With this objective, the acceleration and the maximum velocity (100 mm/s^2 and 20 mm/s, respectively), have been chosen to minimize the acceleration initial transitory. Then, a constant deceleration of 6 mm/s^2 is imposed. This last phase, representative of a braking condition, allows to investigate the relationship between the friction coefficient and the relative velocity.

Regarding the temperature, the trend described in Fig. 8 has been imposed during each test. The temperature law described in Fig. 8 has been conceived to investigate the whole temperature range covered in the investigated application, focusing the attention on 4 different phases: Room Temperature, heating phase, High Temperature (HT) and cooling phase.

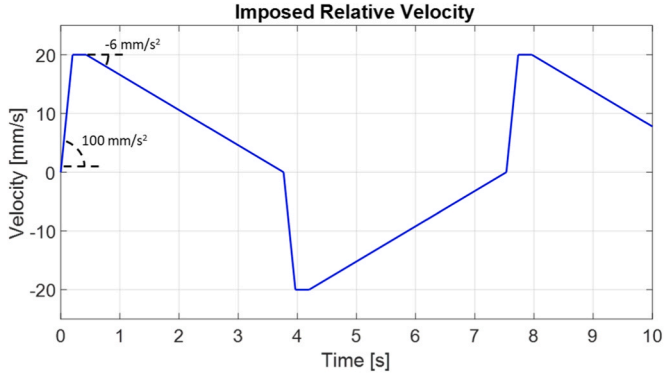

Fig. 7. Variable Velocity imposed motion law. Each stroke is composed by three different phases: 1) Acceleration phase, imposed value 100 mm/s^2; 2) Constant Velocity phase, imposed value 20 mm/s; 3) Deceleration, simulation of braking conditions, imposed value − 6 mm/s^2.

3.2. Example of test post-processing

For each test, the acquired raw data have been processed by MATLAB © to retrieve meaningful information. The main outcomes that have been analyzed are the overall material frictional response, as a function of the imposed temperature (Fig. 9), and a single stroke frictional and dynamic response of the system at high temperature conditions (Fig. 10).

An example of the overall frictional response, measured during a whole test and including about 75 back and forward cycles, in function of the imposed temperature, is reported in Fig. 9. Both normalized friction coefficient (in red) and measured temperature (green) are plotted in function of time. It has been chosen to highlight, in blue, the dynamic friction coefficient, that has been conventionally evaluated as the mean of the friction coefficient values recorded between the 25% and the 50% of each braking stroke (see detail in Fig. 9), correspondent to the part with highest values of sliding velocity, excluding the initial acceleration transitory.

As important as the frictional response, also the correspondent dynamic response of the system (friction-induced vibrations) has been analyzed for the single braking stroke. Fig. 10 presents an example of single-stroke analysis. The analysis focuses here on one single stroke, selected at high temperature conditions, of the reciprocating motion between the samples. By this type of analysis, it can be investigated the evolution of the friction coefficient as a function of the sliding velocity (the velocity decreases from 20 to 0 mm/s during the stroke). The relationship between friction coefficient and relative velocity is, in fact, the key parameter for the occurrence of unstable vibrations caused by negative-slope instability. The vibrational response of the system, consequent to the specific frictional response, is investigated as well by the accelerometer time signal and its normalized spectrogram (short-time Fourier transform, with each window normalized on its maximum value). In the specific stroke reported in Fig. 10, it can be observed as an increase of the friction coefficient with the decrease of the velocity (negative friction-velocity slope) leads to a dynamic instability characterized by an unstable mode that vibrates at its natural frequency. Consequently, the normalized spectrum passes from a broadband spectrum to a harmonic one (at about 549.3 s), corresponding to an increase of the vibration amplitude.

Fig. 11 presents the four different configuration that have been characterized by frictional tests. The baseline material, machined from a used brake disc after service life, has been tested both in its original state (Before US, orange) and without its third body layer, after ultrasonic cleaning (After US, blue). The third body collected on a different disc (3rd body source, green), has been reintroduced on the cleaned sample, used as a substrate. Frictional tests have been performed also on this last configuration (After Reintroduction, black). The performed test sequence allows for a direct comparison between the frictional behavior observed in different configurations, allowing to evaluate the role of the third body (and of the substrate) on the frictional response of the material.

4. Experiment results

In this section, the frictional responses obtained for the different states of the contact samples, described in Section 3, are analyzed, using the post-processing detailed above.

4.1. Frictional tests before US cleaning

The frictional and vibrational response of the reference state has

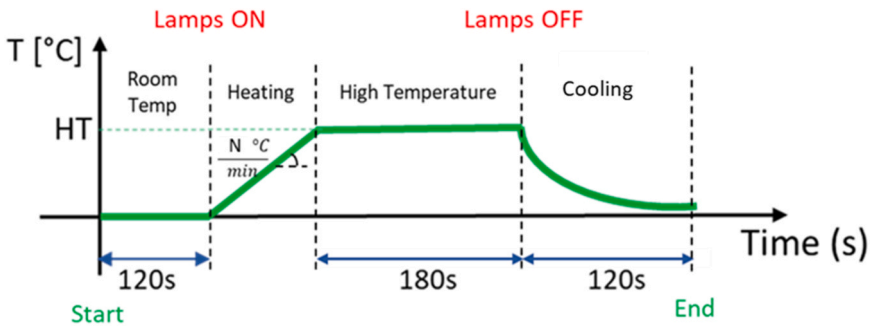

Fig. 8. Imposed Temperature Law. Four different phases have been investigated in each test: Room temperature (RT), Heating, High Temperature (HT), Cooling.

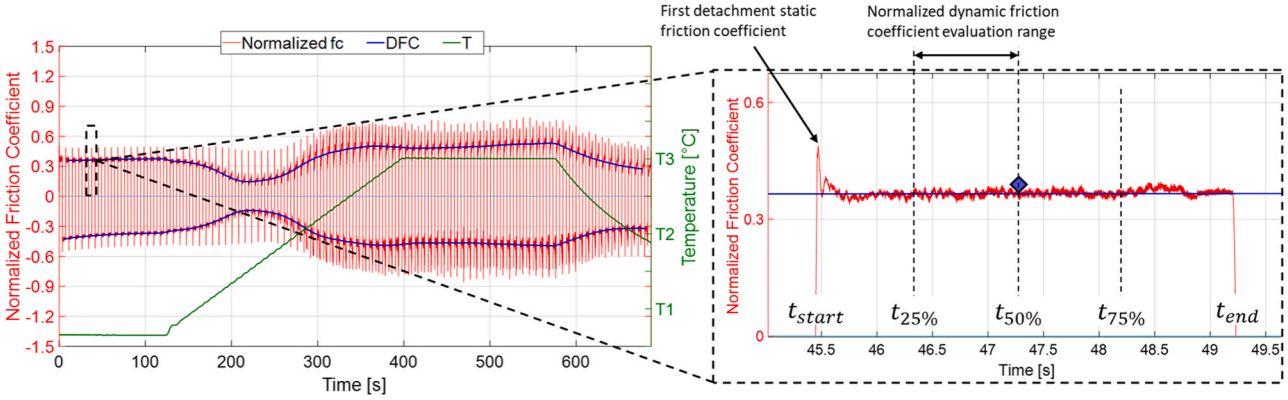

Fig. 9. Plot of the Normalized friction Coefficient (red) and Sample Temperature (green). The normalized Dynamic Friction Coefficient (DFC, blue) and its evaluation range are evidenced.

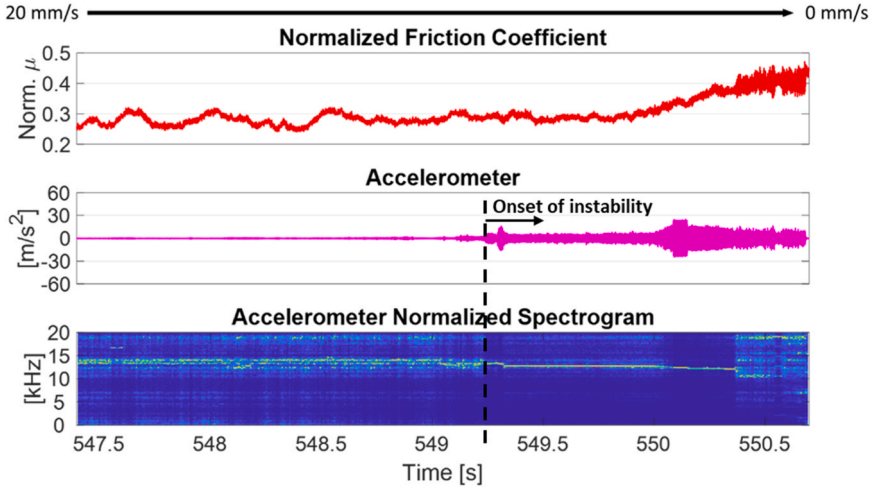

Fig. 10. Example of Single-Stroke analysis. The dynamic response of the system (Accelerometer signal, magenta, and accelerometer normalized spectrogram) is shown with the correspondent frictional response (normalized friction coefficient, red).

been obtained by testing the samples in their original state, after service life. The retrieved frictional response is reported in Fig. 12, as well as the dynamic response observed for a high temperature braking stroke.

As shown in Fig. 12, the friction coefficient strongly depends on the imposed temperature. Different frictional regime can be recognized in correspondence of different temperature conditions:

1. Room Temperature: the contact pair show a constant and reproducible frictional response during the whole room temperature part of the test.
2. Intermediate Temperature (T2): In correspondence of this temperature condition, the friction coefficient approaches a minimum value. This behavior has been already observed in other works that investigated the frictional behavior of similar materials [43,44]. It has been related to the desorption of water vapor from the material bulk and third body layer, registered in these conditions using an in-situ mass spectrometer. The water vapor act as a “lubricant”, lowering the friction coefficient.
3. High Temperature (T3): An abrupt increase of the friction coefficient occurs when passing from temperature T2 towards temperature T3. This behavior, commonly observed for graphitic carbon materials

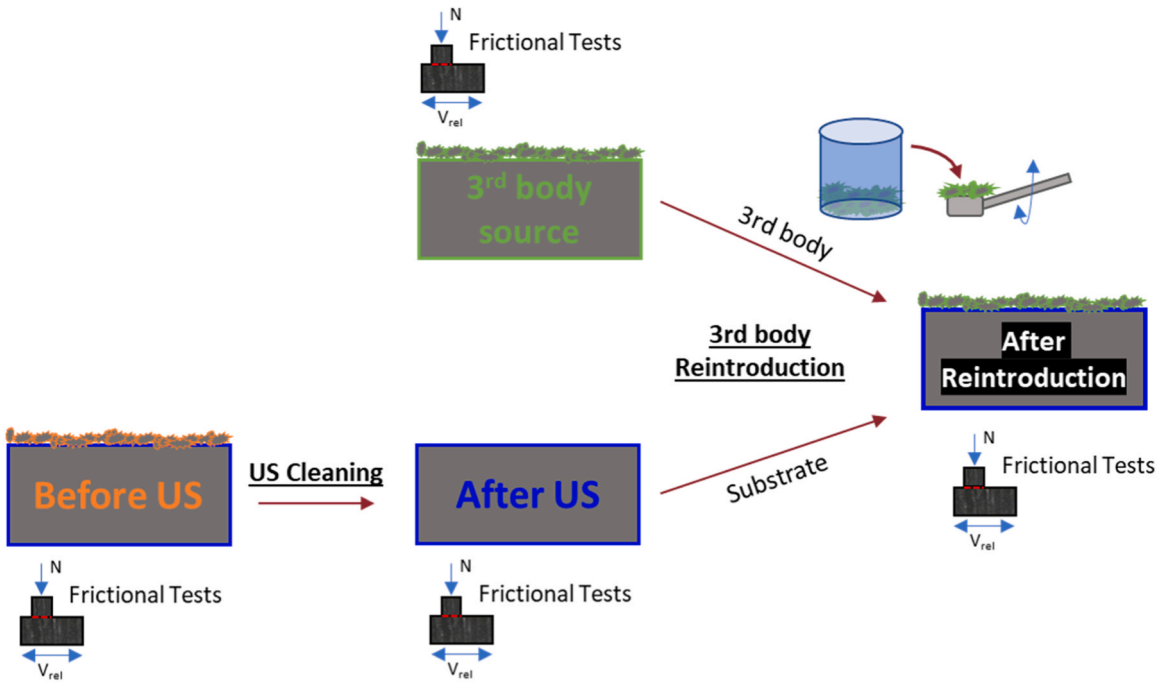

Fig. 11. Sequence of the performed test. Four different configurations have been tested: Before US, After US, Third Body Source, After Reintroduction.

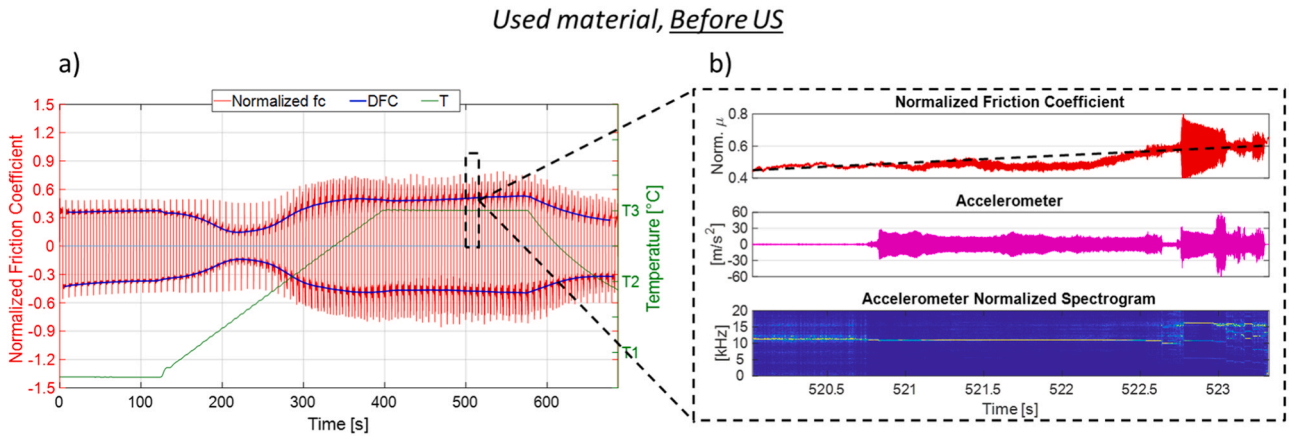

Fig. 12. Global frictional response (a) and high temperature (T3) single-stoke analysis (b). Obtained for baseline material ("Before US", Used conditions).

[27,45], happens because of an increased reactivity of the surfaces in contact, caused by the desorption of chemical species that were able to deactivate the active sites of the material at lower temperatures. In these conditions, therefore, it is privileged a recombination of the active sites between first and third body or, eventually, between the two first bodies in contact, resulting in higher values of the friction coefficient.

To understand the role that third body plays on the frictional behavior of the C/C contact pair, the interface layer, including the contamination elements, has been removed from the surfaces by ultrasonic cleaning.

4.2. *Frictional tests Afterafter US cleaning*

The test presented in the following have been performed on the same samples pair used in 4.1, after having removed the third body layer by the introduced US cleaning procedure. The overall frictional response in function of the temperature, observed after the ultrasonic cleaning (Fig. 13), has been analyzed and compared with the one observed for the material in its original state, before US cleaning, described in Fig. 12.

Comparing Fig. 13a (After US Cleaning) and Fig. 12a (Before US Cleaning), it can be observed that the third body layer almost has almost no influence on the frictional behavior at low temperature, below temperature T2, that appears to be very similar to the one observed before US Cleaning (Fig. 12). Conversely, an important increase of dynamic friction coefficient is observable at high temperature after having removed the third body layer. This behavior could be attributed to a change in the rheological behavior of the third body layer, which "lubricates" the contact, avoiding the direct physicochemical interaction between the two surfaces, which are much stronger at high temperature. Moreover, an increase of the real contact area could contribute as well to the increase of the adhesive contribution of friction [46,47] due to the surface reactivity at higher temperatures.

Comparing the dynamic behaviors (single-stroke analysis) observed before (Fig. 12b) and after US Cleaning (Fig. 13b), it can be observed that the negative friction-velocity slope relationship remarked before US is not observed after ultrasonic cleaning. The high temperature friction

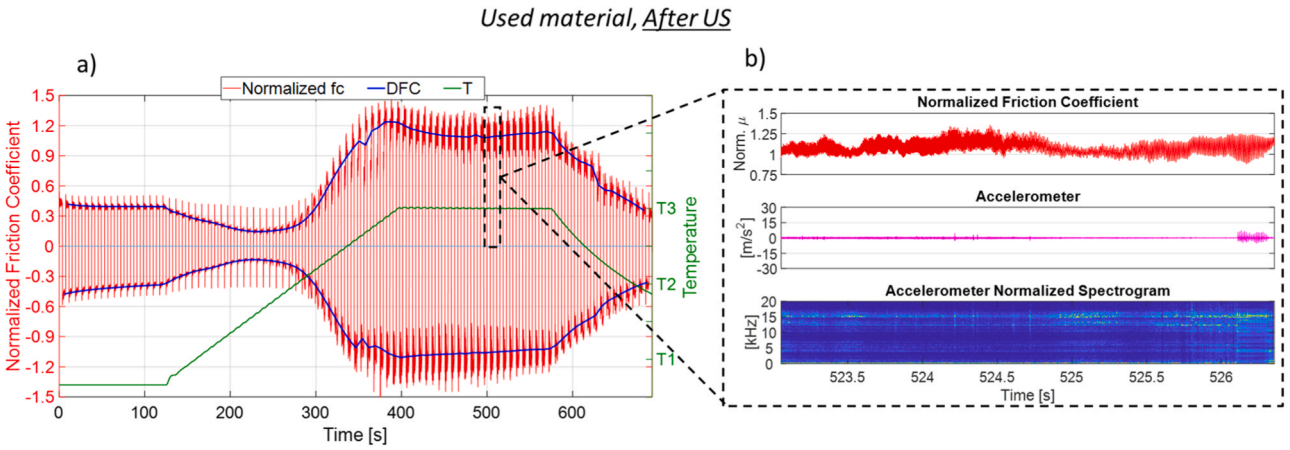

Fig. 13. Global frictional response (a) and high temperature (T_3) single-stoke analysis (b) obtained After US Cleaning. The negative slope $\mu - V_{rel}$ relationship is no more observable.

coefficient, after US cleaning, presents high values and is almost independent from the sliding velocity. Consequently, the dynamic response of the system does not show a negative slope instability.

4.3. Third body reintroduction

One of the objectives of the work consists in the development of an experimental procedure to (re)introduce an external third body on a substrate obtained from a used material, previously cleaned of its own third body by US cleaning. This procedure could allow to test different third bodies maintaining a substrate representative of the operative conditions. The procedure described in 2.4 has been applied using the third body recovered from a different brake disc than the one of the substrate. This material will be referred as "Third Body source". Fig. 14b shows the frictional response obtained after third body reintroduction. The behavior observed for the substrate after US cleaning, in absence of the third body layer, is reported as a comparison (Fig. 14a).

As shown in Fig. 14, the reintroduction of third body on the cleaned samples drastically lowered the friction coefficient at high temperatures, if compared with the situation observed after US cleaning (Fig. 13). The obtained values of the friction coefficient at high temperature are even lower than the ones observed for the sample from which the substrate comes (before US Cleaning, Fig. 12). To understand this behavior, it has been chosen to perform frictional test also on a sample pair machined from the material "third body source", from which the third body comes. Fig. 15 presents a comparison of the results obtained for the three different conditions: a) frictional response of the substrate material before US cleaning; b) frictional response of the substrate cleaned samples with reintroduced third body; c) frictional response of the sample from which the third body has been recovered (Third body source).

As shown in Fig. 15, the frictional behavior of the "Substrate + Reintroduced 3rd body" configuration is much more similar to the behavior of the "Third body source" material, rather than to the one of the substrate before cleaning. This result underlines the importance of third body role on the frictional performance of the contact pair, in this case more important than the first bodies (substrates).

Comparing the single strokes at high temperature, as shown in Fig. 16, the similarity is confirmed even in terms of dependance of the friction coefficient on the sliding velocity.

Looking at Fig. 16, it is remarkable that, at high temperature conditions, the frictional behavior of the material source of third body, before cleaning, is almost identical to the one of the Substrate with the Reintroduced third body. Moreover, the same dependance of the friction coefficient in function of the sliding velocity is observed, with a strong negative friction-velocity slope relationship.

Conversely, the comparison between strokes selected at room temperature conditions, evidences the lower importance of the third body rheology on the frictional response of the contact pair in these conditions. As shown in Fig. 17, similar values of the friction coefficient have been observed at room temperature conditions for all the analyzed configurations.

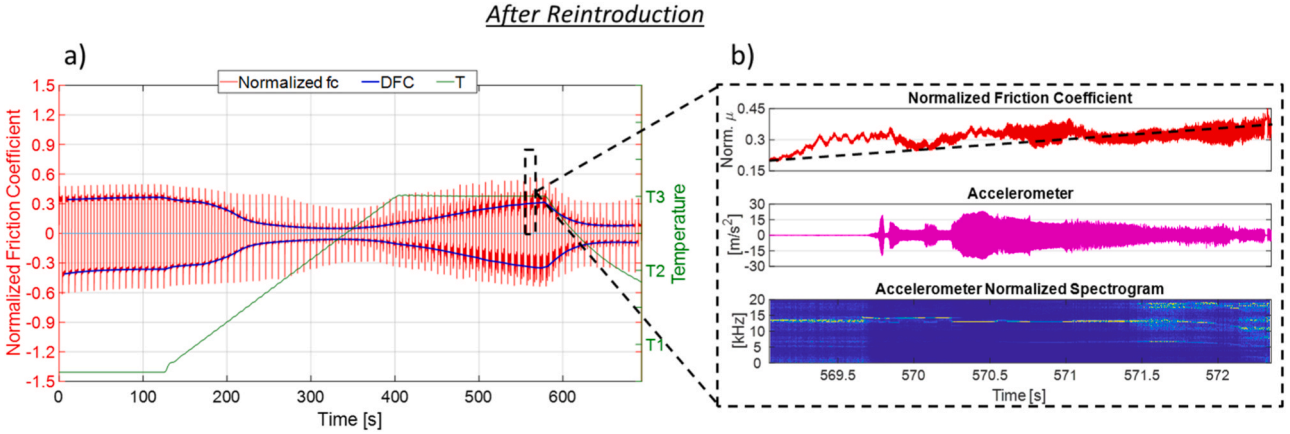

Fig. 14. Global frictional response (a) and high temperature (T3) single-stoke analysis (b). Obtained after third body reintroduction (Substrate after US cleaning + Reintroduced third body).

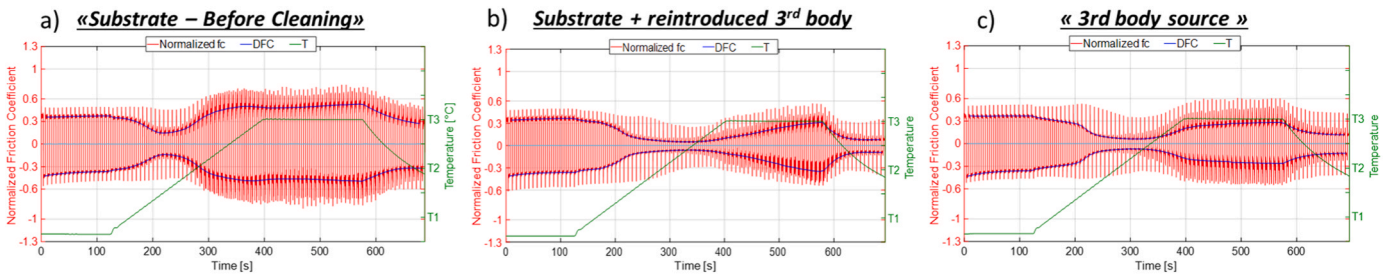

Fig. 15. Comparison of the global frictional response in function of the temperature: a) Substrate material Before US Cleaning b) Substrate + Reintroduced 3rd body c) Third Body source material. The frictional behavior of the mix Substrate + Reintroduced third body is very similar to the behavior of the material source of 3rd body.

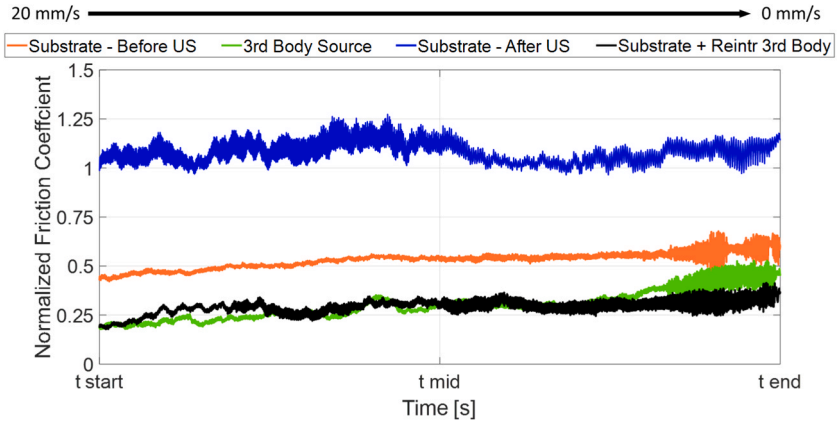

Fig. 16. Comparison of single strokes at high temperature (T3) conditions. Four different tests are compared: Substrate - Before US (orange), Third body source (Green), Substrate - After US (Blue), Substrate + 3rd body reintroduction (Black).

5. Discussion / Conclusion

The procedure proposed in this work allows to perform frictional tests maintaining the same substrate (first bodies) and changing the interface layer (third body). As a consequence, direct comparison between successive tests can be performed to retrieve meaningful information about the third body role on the frictional behavior of the material.

A C/C contact pair has been analyzed by the use of the described approach, characterizing the frictional and dynamic response under different temperature conditions. The main results are listed in the following:

- For the tested C/C material, the effect of third body is almost unappreciable at low temperatures, as shown by the similar values of the friction coefficient observed, at low temperature, before and after US cleaning, as well as after the third body reintroduction on surfaces. Conversely, at high temperatures, when the reactivity of the material is increased, the third body strongly affect the frictional performance of the material. This different behavior can be explained by the complexity of the rheology of the third body layer, which can be largely affected by its physiochemical reactivity at higher temperatures.
- The third body strongly influences the frictional performance of the contact pair, more than the first bodies. After 3rd body

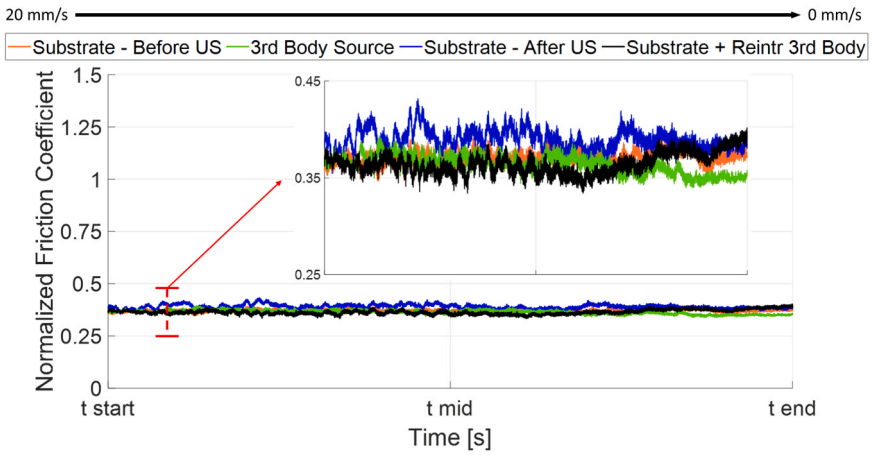

Fig. 17. Comparison of single strokes at room temperature conditions. Four different tests are compared: Substrate - Before US (orange), Third body source (Green), Substrate - After US (Blue), Substrate + 3rd body reintroduction (black).

reintroduction, the frictional material response of the substrate with the reintroduced third body has been observed to be much more similar to the one of the contact pair source of the third body, rather than to the one of the substrate before cleaning. It could be deduced, then, that the frictional performances are almost governed by the third body layer, pointing out a strong influence of material physiochemistry for the analyzed C/C contact pair.

- More in general, meaningful information can be obtained by the (re)introduction of an external third body on a used substrate, previously cleaned of its own third body by ultrasonic cleaning. As a result, the developed procedure, can be applied to test external / artificial third bodies (e.g. different morphologies, different chemical compositions) reintroduced on a substrate representative of first body encountered in the operative conditions.

The presented results and the proposed methodology open the way to investigate the effect of different third body features and compositions on the frictional and dynamic response of contact pairs.

Declaration of Competing Interest

The authors declare that they have no known competing financial interests or personal relationships that could have appeared to influence the work reported in this paper.

Data availability

The data that has been used is confidential.

Acknowledgements

The authors gratefully acknowledge the French National Research and Technology Association (ANRT) and Safran Landing Systems, CIFRE convention 2022/0290, for supporting this research project.

References

[1] Godet M. The third-body approach: a mechanical view of wear. fasc. 1–3 Wear 1984;vol. 100:437–52.
[2] Berthier Y. Experimental evidence for friction and wear modelling (lug) Wear 1990;vol. 139(fasc. 1):77–92. https://doi.org/10.1016/0043-1648(90)90210-2.
[3] Godet M, Play D, Berthe e D. An attempt to provide a unified treatment of tribology through load carrying capacity, transport, and continuum mechanics. J Lubr Technol 1980;vol. 102(fasc. 2):153–64. https://doi.org/10.1115/1.3251457.
[4] Berthier Y, Godet M, Brendle e M. Velocity accommodation in friction (gen) Tribol Trans 1989;vol. 32(fasc. 4):490–6. https://doi.org/10.1080/10402008908981917.
[5] Renouf M, Cao H-P, Nhu e V-H. Multiphysical modeling of third-body rheology (fasc) Tribol Int 2011;vol. 44(4):417–25. https://doi.org/10.1016/j.triboint.2010.11.017.
[6] Zhang Y, Mollon G, Descartes e S. Significance of third body rheology in friction at a dry sliding interface observed by a multibody meshfree model: Influence of cohesion between particles. Tribol Int 2020;vol. 145:106188. https://doi.org/10.1016/j.triboint.2020.106188.
[7] Godet e Y. Berthier M. Continuity and dry friction: An Osborne Reynolds approach. in Tribology Series, vol. 11. Elsevier; 1987. p. 653–61. https://doi.org/10.1016/S0167-8922(08)70999-4.
[8] Lyashenko IA, Li Q, Popov e VL. Influence of chemical heterogeneity and third body on adhesive strength: experiment and simulation ([Online]. Disponibile su: https://www.frontiersin.org/articles/) Front Mech Eng 2021;vol. 7. https://doi.org/10.3389/fmech.2021.658858.
[9] Willert E. Self-consistency conditions in static three-body elastic tangential contact. Facta Univ Ser Mech Eng, Mag 2021. https://doi.org/10.22190/FUME210306038W.
[10] Akay A. Acoustics of friction (fasc) J Acoust Soc Am 2002;vol. 111(4):1525–48. https://doi.org/10.1121/1.1456514.
[11] Ibrahim RA. Friction-induced vibration, chatter, squeal, and chaos—part I: mechanics of contact and friction (fasc) Appl Mech Rev 1994;vol. 47(7):209–26. https://doi.org/10.1115/1.3111079.
[12] Tonazzi D, Massi F, Baillet L, Brunetti J, Berthier e Y. Interaction between contact behaviour and vibrational response for dry contact system. Mech Syst Signal Process 2018;vol. 110:110–21.
[13] Singla N, Brunel J-F, Mège-Revil A, Kasem H, Desplanques e Y. Experiment to investigate the relationship between the third-body layer and the occurrence of squeals in dry sliding contact (fasc) Tribol Lett 2020;vol. 68(1):4. https://doi.org/10.1007/s11249-019-1244-x.
[14] Sinou e L. Jézéquel J-J. Mode coupling instability in friction-induced vibrations and its dependency on system parameters including damping (fasc) Eur J Mech - ASolids 2007;vol. 26(1):106–22. https://doi.org/10.1016/j.euromechsol.2006.03.002.
[15] Lazzari A, Tonazzi D, Massi e F. Squeal propensity characterization of brake lining materials through friction noise measurements. Mech Syst Signal Process 2019;vol. 128:216–28. https://doi.org/10.1016/j.ymssp.2019.03.034.
[16] Kang J, Krousgrill CM, Sadeghi e F. Comprehensive stability analysis of disc brake vibrations including gyroscopic, negative friction slope and mode-coupling mechanisms (fasc) J Sound Vib 2009;vol. 324(1):387–407. https://doi.org/10.1016/j.jsv.2009.01.050.
[17] Papangelo A, Ciavarella M, Hoffmann e N. Subcritical bifurcation in a self-excited single-degree-of-freedom system with velocity weakening–strengthening friction law: analytical results and comparison with experiments (fasc) Nonlinear Dyn 2017;vol. 90(3):2037–46. https://doi.org/10.1007/s11071-017-3779-4.
[18] Tonazzi D, Massi F, Baillet L, Culla A, Di Bartolomeo M, Berthier e Y. Experimental and numerical analysis of frictional contact scenarios: from macro stick–slip to continuous sliding (fasc) Meccanica 2015;vol. 50(3):649–64.
[19] Lazzari A, Tonazzi D, Conidi G, Malmassari C, Cerutti A, Massi e F. Experimental evaluation of brake pad material propensity to stick-slip and groan noise emission (fasc) Lubricants 2018;vol. 6(4):107.
[20] Manocha LM. High performance carbon-carbon composites (fasc) Sadhana 2003;vol. 28(1):349–58. https://doi.org/10.1007/BF02717143.
[21] Windhorst e G. Blount T. Carbon-carbon composites: a summary of recent developments and applications (fasc) Mater Des 1997;vol. 18(1):11–5. https://doi.org/10.1016/S0261-3069(97)00024-1.
[22] Burchell TD. Carbon materials for advanced technologies. Elsevier; 1999.
[23] Devi e K. R. Rao GR. Carbon-carbon composites -an overview. Def Sci J 1993;vol. 43:369–83.
[24] Chen e C. P. Ju JD. Effect of sliding speed on the tribological behavior of a PAN-pitch carbon-carbon composite (fasc) Mater Chem Phys 1995;vol. 39(3):174–9. https://doi.org/10.1016/0254-0584(94)01427-I.
[25] Chen JD, Chern Lin JH, Ju e CP. Effect of humidity on the tribological behavior of carbon-carbon composites (fasc) Wear 1996;vol. 193(1):38–47. https://doi.org/10.1016/0043-1648(95)06667-5.
[26] Gomes JR, Silva OM, Silva CM, Pardini LC, Silva e RF. The effect of sliding speed and temperature on the tribological behaviour of carbon–carbon composites (fasc) Proc Ninth Nord Symp Tribol 2001;vol. 249(3):240–5. https://doi.org/10.1016/S0043-1648(01)00554-3.
[27] YEN BK, ISHIHARA T, YAMAMOTO e I. Influence of environment and temperature on “dusting” wear transitions of carbon–carbon composites (fasc) J Mater Sci 1997;vol. 32(3):681–6. https://doi.org/10.1023/A:1018539819346.
[28] Yen BK. Influence of water vapor and oxygen on the tribology of carbon materials with sp2 valence configuration (fasc) Wear 1996;vol. 192(1):208–15. https://doi.org/10.1016/0043-1648(95)06807-4.
[29] Di Bartolomeo M, Lazzari A, Stender M, Berthier Y, Saulot A, Massi e F. Experimental observation of thermally-driven frictional instabilities on C/C materials. Tribol Int 2021;vol. 154:106724.
[30] Lazzari A, Tonazzi D, Brunetti J, Saulot A, Massi e F. Contact instability identification by phase shift on C/C friction materials. Mech Syst Signal Process 2022;vol. 171:108902. https://doi.org/10.1016/j.ymssp.2022.108902.
[31] Hutton TJ, McEnaney B, Crelling e JC. Structural studies of wear debris from carbon–carbon composite aircraft brakes (fasc) Carbon 1999;vol. 37(6):907–16.
[32] Pevida C, Jacquemard P, Joly e J-P. Physicochemical properties of debris ejected from C/C brakes with different structural orders (fasc) Carbon 2008;vol. 46(7):994–1002.
[33] Lei B, et al. New insights into the microstructure of the friction surface layer of C/C composites (fasc) Carbon 2011;vol. 49(13):4554–62. https://doi.org/10.1016/j.carbon.2011.06.073.
[34] Ozcan e P. Filip S. Microstructure and wear mechanisms in C/C composites (fasc) Wear 2005;vol. 259(1–6):642–50.
[35] Lacerra G, Di Bartolomeo M, Milana S, Baillet L, Chatelet E, Massi e F. Validation of a new frictional law for simulating friction-induced vibrations of rough surfaces. Tribol Int 2018;vol. 121:468–80. https://doi.org/10.1016/j.triboint.2018.01.052.
[36] Di Bartolomeo M, Lacerra G, Baillet L, Chatelet E, Massi e F. Parametrical experimental and numerical analysis on friction-induced vibrations by a simple frictional system. Tribol Int 2017;vol. 112:47–57.
[37] Mason TJ. Ultrasonic cleaning: An historical perspective. Ultrason Sonochem 2016;vol. 29:519–23. https://doi.org/10.1016/j.ultsonch.2015.05.004.
[38] Ghezzi I, Tonazzi D, Rovere M, Le Coeur C, Berthier Y, Massi e F. Frictional behaviour of a greased contact under low sliding velocity condition. Tribol Int 2021;vol. 155:106788.
[39] Wong PL, Bullough WA, Feng C, Lingard e S. Tribological performance of a magneto-rheological suspension (fasc) Wear 2001;vol. 247(1):33–40. https://doi.org/10.1016/S0043-1648(00)00507-X.
[40] Mofidi M, Kassfeldt E, Prakash e B. Tribological behaviour of an elastomer aged in different oils (fasc) Nord 2006 2008;vol. 41(9):860–6. https://doi.org/10.1016/j.triboint.2007.11.013.
[41] Ghassemi MH, Abouei V, Moshtaghi M, Noghani e MT. The effect of removing worn particles by ultrasonic cleaning on the wear characterization of LM13 alloy (fasc) Surf Eng Appl Electrochem 2015;vol. 51(4):382–8. https://doi.org/10.3103/S1068375515040067.

[42] Ilie F, Covaliu e C. Tribological properties of the lubricant containing titanium dioxide nanoparticles as an additive (fasc) Lubricants 2016;vol. 4(2). https://doi.org/10.3390/lubricants4020012.
[43] Gouider M, Berthier Y, Jacquemard P, Rousseau B, Bonnamy S, Estrade-Szwarckopf e H. Mass spectrometry during C/C composite friction: carbon oxidation associated with high friction coefficient and high wear rate (fasc) Wear 2004;vol. 256(11):1082–7. https://doi.org/10.1016/S0043-1648(03)00534-9.
[44] Brender P, et al. Characterization of carbon surface chemistry by combined temperature programmed desorption with in situ X-ray photoelectron spectrometry and temperature programmed desorption with mass spectrometry analysis (fasc) Anal Chem 2012;vol. 84(5):2147–53. https://doi.org/10.1021/ac102244b.
[45] Lancaster e J. Pritchard J. On the “dusting” wear regime of graphite sliding against carbon. J Phys Appl Phys 2000;vol. 13:1551. https://doi.org/10.1088/0022-3727/13/8/025.
[46] McFarlane JS, Tabor D, Bowden e FP. Relation between friction and adhesion (fasc) Proc R Soc Lond Ser Math Phys Sci 1997;vol. 202(1069):244–53. https://doi.org/10.1098/rspa.1950.0097.
[47] Lyashenko e V. L. Popov IA. The influence of adhesion on rolling and sliding friction: an experiment (fasc) Tech Phys 2022;vol. 67(3):203–14. https://doi.org/10.1134/S106378422204003X.